Proceedings of the ASME 2011 Internal Combustion Engine Division Fall Technical Conference
ICEF2011
October 2-5, 2011, Morgantown, West Virginia, USA

ICEF2011-60122

THE EFFECTS OF FUEL CHARACTERISTICS ON STOICHIOMETRIC SPARK-ASSISTED HCCI

Adam J. Weall and James P. Szybist
Fuels, Engines and Emissions Research Center
Oak Ridge National Laboratory
NTRC Building, 2360 Cherahala Blvd., Knoxville, TN, USA

ABSTRACT

The characteristics of fuel lean HCCI operation using a variety of fuels are well known and have been demonstrated using different engine concepts in the past. In contrast, stoichiometric operation of HCCI is less well documented. Recent studies have highlighted the benefits of operating at a stoichiometric condition in terms of load expansion combined with the applicability of three way catalyst technology to reduce NOx emissions.

In this study the characterization of stoichiometric HCCI using gasoline-like fuels was undertaken. The fuels investigated are gasoline, a 50 vol% blend of iso-butanol and gasoline (IB50), and an 85% vol blend of ethanol and gasoline (E85). A single cylinder engine operating with direct injection and spark assist combined with a fully variable hydraulic valve actuation system allowed a wide range of operating parameters to be studied.

This included the effects of negative valve overlap duration, intake valve closing and valve lift. Furthermore, the interaction between fuel injection timing and spark and how they can affect the required valve timing to achieve stoichiometric HCCI combustion are also studied.

A comprehensive combustion and emissions analysis is conducted using gasoline, IB50 and E85 at an engine speed of 2000rpm over a range of operating loads.

The resultant fuel properties which differed in terms of octane rating, fuel oxygenation and heat of vaporization show that stoichiometric HCCI is possible using a range of fuels but that these fuel characteristics do have some effect on the combustion characteristics. How these fuel properties can enable an increased engine operating envelope to be achieved, in comparison with both fuel lean HCCI and conventional spark ignited combustion, is then discussed.

INTRODUCTION

Reducing petroleum consumption is in our national interests because it reduces dependence on foreign oil while reducing our anthropogenic carbon dioxide emissions. Reductions can be achieved in multiple ways, including through increasing the efficiency of internal combustion engines and by direct displacement of petroleum with renewable fuels. Both of these strategies are part of the US Department of Energy Multi-Year Program Plan for the Vehicle Technologies program [1], and both strategies are addressed in this study.

During the past 10-15 years a number of combustion concepts have been researched in order to reduce engine-out emissions and increase efficiency. These include homogeneous charge compression ignition (HCCI), premixed charge compression ignition (PCCI) and low temperature combustion (LTC). These approaches share a similar approach, to operate under dilute conditions at low combustion temperatures with minimal fuel-air stratification.

HCCI, demonstrated in a gasoline fueled 4-stroke engine 28 years ago [2] has yet to enter production due to a number of factors. Barriers to implementation included robust control strategies and sensors, transient operation, valvetrain constraints and a limited operating load range.

HCCI operation is limited to part-load conditions due to high rates of in-cylinder pressure rise rate, making it applicable to only a small portion of the engine map. The higher efficiency at

part-load conditions is challenged by the growth of hybrid-electric powertrains in production vehicles, which minimize the use of the engine at the lowest engine loads and operate the engine at more efficient higher-load conditions whenever possible. Thus, if HCCI is to remain a relevant means of increasing efficiency, there is a need for a greater emphasis on expanding the operating regime to higher load.

HCCI combustion can be achieved with the use of variable valve timing to produce negative valve overlap (NVO). NVO is achieved by closing the exhaust valves earlier than in conventional engines, thereby trapping a portion of the exhaust gases in-cylinder and recompressing them for the remainder of the exhaust stroke. The intake valve is then opened later than in a conventional engine so that the re-compressed exhaust can be expanded.

Functionally, NVO allows large amounts of hot exhaust gas residuals (EGR) to be retained in-cylinder for the following engine cycle. Compared to conventional SI combustion, efficiency and emissions benefits of NVO HCCI have been demonstrated in for example [3].

A promising approach to increase the high load operating limit of NVO HCCI is to produce a spark-ignited flame front followed by a volumetric combustion event, or auto-ignition event throughout the remaining unburned regions in the cylinder in the same manner that HCCI combustion occurs. This type of mixed-mode combustion has been examined by a number of researchers under names such as spark-ignited compression ignition (SI-CI) [4], spark-assisted HCCI [5],[6],[7] and spark-assisted compression ignition (SACI) [8],[9],[10]. This use of spark-assistance does differ somewhat from the use of spark events during mode transitions between SI and HCCI in for example [11], where the spark is used to provide combustion stability during the transition.

One consequence of operating in this mixed-mode combustion strategy at higher loads is that emissions of oxides of nitrogen (NO_x) can be increased by several orders of magnitude. In the study of [12] it is confirmed that an increase in IMEP could be achieved with the use of spark assist but that increases in emissions of oxides of nitrogen could be seen.

Under stoichiometric condition, very low tailpipe-out NO_x emissions can be achieved regardless of engine-out NO_x emissions. The low tail-pipe out NO_x emissions are possible because of mature three-way catalyst technology. Thus, expansion of the engine load limit can be achieved without being limited by high engine-out NO_x emissions. Stoichiometric operation of spark-assisted HCCI (SA-HCCI) has been demonstrated in [5],[6],[7],[8],[10].

Independent of the development of advanced combustion strategies like stoichiometric spark-assist HCCI is an increasing emphasis on the use of alternative fuels. The growth can be attributed in a large part to the Energy Independence Security Act (EISA) which, requires by law, aggressive increases in the use of these fuels. Ethanol is by far the most significant biofuel currently in use for spark-ignition engines, with infrastructure in-place and E10 and E85 being consumed on large scales. More recently, research into longer chain alcohols has increased, with iso-butanol being of particular interest.

The low energy density of ethanol results in a substantial fuel economy difference between gasoline and E85, which poses a significant barrier to more widespread use. Compared to ethanol, iso-butanol has an energy density that is more similar to gasoline. In addition, iso-butanol is less hydrophilic than ethanol which may make it more compatible with existing gasoline infrastructure.

The purpose of this paper is to investigate fuel effects under stoichiometric SA-HCCI. The study includes three fuels: gasoline, E85, and a 50% gasoline to 50% iso-butanol blend. The focus is to characterize the operable load range at 2000rpm with these fuels, and to investigate the authority of the valvetrain, spark, and fuel injection timing to control the combustion event.

FUEL PROPERTIES

Three test fuels are used in this study: an emissions certification gasoline (UTG91), a 50/50 by volume blend of UTG91 and iso-butanol (IB50), and a blend of 85% ethanol and 15% by volume gasoline-range hydrocarbons (E85). The iso-butanol (2-methyl-1-propanol) has an ACS reagent-grade purity of ≥99%. The iso-butanol and UTG91 are splash-blended on site whereas the E85 is purchased pre-blended. The fuel properties are given in table 1. The fuel properties of pure iso-butanol and ethanol are given in table 2 for reference.

TABLE 1 FUEL PROPERTIES: TEST FUELS

	UTG91	IB50	E85
Carbon wt/%	86.2	74.7	55.9
Hydrogen wt/%	13.8	13.4	13.0
Oxygen wt/%	0	11.3	31.1
Density/kg/m^3	739	778.7	786
Octane nr (R+M)/2	86.8	94	96.9
RON/-	90.8	101	105
MON/-	82.7	87	88.7
(RON-MON)/-	8.1	14	16.3
Lower heating value/MJ/kg	43.5	37.6	28.7
Energy density/MJ/l	32.1	29.3	22.6
Stoichiometric AFR/-	14.6	12.7	9.5

TABLE 2 FUEL PROPERTIES: ISO-BUTANOL AND ETHANOL

	Iso-butanol	Ethanol
Chemical formula	$C_4H_{10}O$	C_2H_6O
Oxygen mass/%	21.6	34.8
Density/kg/m^3	801.8 [13]	785.22 [14]
Octane nr (R+M)/2	99.5	116
RON/-	109 [13]	129 [13]
MON/-	90 [13]	103 [13]
(RON-MON)/-	19	26
Lower heating value/MJ/kg	32.959	26.75 [15]
Energy density/MJ/l	26.4	21
Stoichiometric AFR/-	11.1	9

EXPERIMENTAL SETUP

A highly modified GM 2.0L Ecotec engine with direct fuel injection is used for the study. The engine geometry is listed in table 3. Three of the cylinders of the production engine are disabled to allow single-cylinder operation, a custom piston is installed to increase compression ratio to 11.85, and the engine is operated naturally aspirated without external EGR.

The engine used in this study is equipped with a hydraulic valve actuation (HVA) system to enable fully variable valve actuation. Machining modifications have been made to the cylinder head to accommodate the small research module HVA system from Sturman Industries. Modifications include using custom intake and exhaust valves with longer valve stems. While the valve material is different than the production valves, the combustion chamber geometry is unchanged.

TABLE 3 ENGINE GEOMETRY

Bore x Stroke	86mm x 86mm
Conrod length	145.5mm
Compression ratio	11.85:1
Fuel injection system	Direct injection, wall guided

Other changes to the engine include a custom exhaust system and a Kistler sparkplug with an integrated piezoelectric pressure transducer. A picture of the engine is shown in fig. 1.

Drivven Combustion Analysis Toolkit (DCAT) performs the crank-angle resolved data acquisition and combustion analysis. These measurements include cylinder pressure, valve lift feedback from each of the four valves and current sent to the fuel injector. Crank-angle resolved data is recorded at 0.2degCA intervals over 300 consecutive cycles, and all references to indicated mean effective pressure (IMEP) refer to net IMEP. Post-processing and averaging methods are described in the text.

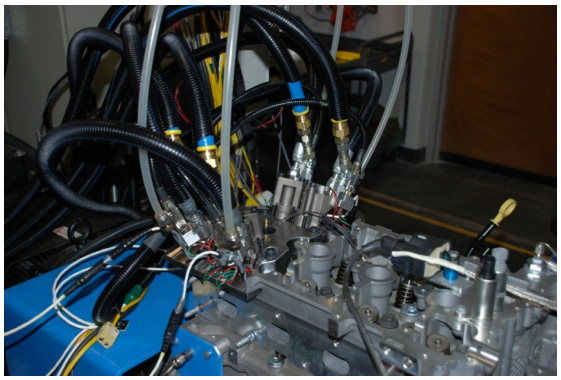

FIGURE 1 TEST ENGINE

Engine emissions are measured using a standard emissions bench. NO_X is measured using a chemiluminescence analyzer, CO and CO_2 are measured using infrared analyzers, oxygen is measured using a paramagnetic analyzer and unburned hydrocarbon emissions (HC) are measured with a flame ionization detector. Smoke measurements are performed using a filter smoke number (FSN) instrument. Exhaust air-to-fuel ratio (AFR) is measured using both gaseous emissions and a wideband exhaust lambda sensor.

Air mass flow is measured using a laminar flow element device and fuel flow is measured using a coriolis-effect based flow meter. Fuel rail pressure is regulated to a constant 95 bar using a process pump with a closed-loop electro-pneumatically controlled pressure regulator. Engine coolant is maintained at 100°C. The air supplied to the engine intake manifold is externally conditioned to 55% relative humidity and 25°C using an air supply conditioning unit. The intake air temperature in this paper is measured inside the intake manifold before the intake port. The exhaust temperature is measured in the exhaust manifold directly after the exhaust port.

EXPERIMENTAL PROCEDURE

The approach to stoichiometric spark-assisted homogeneous charge compression ignition (SA-HCCI) in this study builds on an earlier investigation [7] by the authors. NVO is employed to provide internal EGR and raise the in-cylinder temperature during the compression stroke.

A mixed mode of combustion is initiated with ignition from a conventional spark plug which leads to a flame propagation controlled combustion event before the onset of volumetric combustion. The magnitude of the flame propagation phase depends on several factors including NVO duration, fuel injection timing and spark timing.

In this investigation, engine speed is limited to 2000 rpm. The experimental test matrix consisted of variation of NVO duration as well as DI and spark timing in order to examine the combustion characteristics of the test fuels from the low load limit to the high load limit. The application of late intake valve closing (LIVC) is applied at several operating points in order to control the in-cylinder pressure rise rate.

During most operating points in the spark-assisted HCCI regime studied in this paper a significant proportion of heat release occurred during the initial spark-ignited propagating flame event. This was then followed by auto-ignition dominated heat release.

In order to quantify this ratio it was assumed that the transition point between these two combustion events was related to the inflexion point observed in the crank angle resolved rate of heat release. This ratio, termed the 'initial slow heat release' (ISHR) is discussed in further detail in the annex section.

RESULTS

ENGINE-OUT EMISSIONS

The combustion regime reported in this study is stoichiometric. Therefore emissions of CO_2 and CO are elevated at levels of approximately 15% and 3000-5000ppm respectively depending on operating point and fuel.

The levels of engine-out NO_x emission are reduced when compared with conventional SI combustion. To illustrate this, a selection of operating points covering three operating loads operating in conventional spark ignition mode and in spark assisted HCCI mode are compared in terms of indicated specific NO_x at an engine speed of 2000rpm, shown in fig.2. Similar findings regarding NO_x emissions at increased operating loads during SA-HCCI were reported in [6]. Some reduction is observed for the oxygenated fuels and in particular for E85. However, these engine-out levels can exceed 1000ppm in magnitude at the high load limit.

Hydrocarbon emissions are found to be of the order of 800-2000ppm depending on operating point and fuel with some reduction again seen with the oxygenated fuels, shown in fig. 3 where indicated specific HC is plotted for the same data points shown in fig. 2. The exhaust temperature remained above 380°C, which is sufficiently high to maintain functionality of 3-way catalysts.

A lower combustion temperature can explain NO_x reduction and differences in fuel characteristics can explain HC reductions. The presence of components boiling at higher temperatures in gasoline fuel is expected to increase HC emissions in comparison with ethanol, [16].

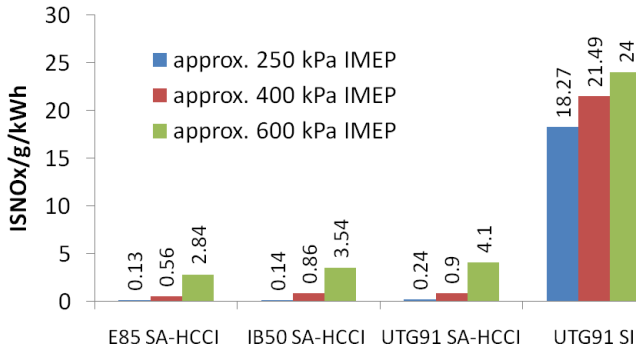

FIGURE 2 ENGINE-OUT INDICATED SPECIFIC NO_X EMISSIONS (SA-HCCI AND SI)

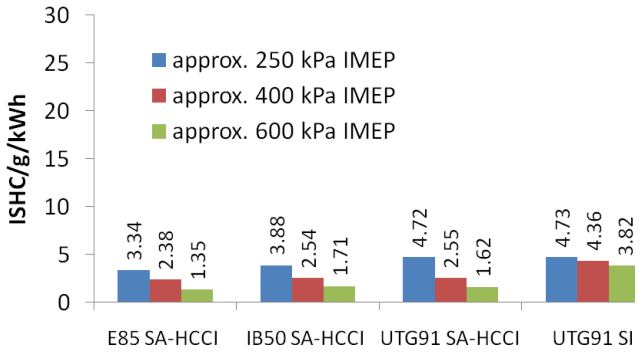

FIGURE 3 ENGINE-OUT INDICATED SPECIFIC HC EMISSIONS (SA-HCCI AND SI)

Throughout the SA-HCCI regime examined here, from 250 kPa IMEP to 700 kPa IMEP filter smoke emissions remain low for all fuels, although the smoke emissions are highest for the UTG91 fuel. This is illustrated in table 4 showing the maximum smoke emissions for the SA-HCCI operating regime examined. These smoke levels are comparable or below smoke levels with production GDI vehicles.

TABLE 4 MAXIMUM SMOKE EMISSIONS (SA-HCCI)

	FSN/IMEP
UTG91	0.084 FSN @ 600kPa
IB50	0.008 FSN @ 627kPa
E85	0.005 FSN @ 707kPa

In summary, gaseous emissions under SA-HCCI conditions are at or below levels measured during SI combustion for all fuels. Emission levels do exhibit fuel dependencies; with E85 producing the lowest levels of HC and NOx emissions. Emissions from all fuels are sufficiently high to require

aftertreatment with a 3-way catalyst, and thus no differences are expected in tailpipe-out gaseous emissions.

Finally it is found that smoke emissions are low for all fuels during the SA-HCCI regime, as quantified by FSN, but that the emissions for UTG91 are higher than for the oxygenated fuels, with E85 exhibiting the lowest measurements both during SA-HCCI and SI combustion regimes.

COMBUSTION CHARACTERISTICS

The combustion characteristics and how the different fuels examined here affect the combustion behavior will be discussed in the following sections.

Light Engine Loads (≈380-400 kPa IMEP region)

At operating loads approaching 400kPa IMEP at 2000 rpm, lean HCCI becomes limited by NO_x and pressure rise rate considerations [17]. Stoichiometric SA-HCCI allows this boundary to be crossed as a consequence of the applicability of a 3-way catalyst for NOx mitigation. The effect of stoichiometric operation with spark-assistance on pressure rise rates at this transition region is discussed in combination with fuel effects.

At this operating load region an increased NVO duration (220degCA) and a low valve lift (4mm) are necessary in order to reduce the charge air mass to achieve stoichiometric combustion. A consequence of this is a high level of trapped residual mass and a higher bulk gas temperature during the compression stroke. At this operating point, stoichiometric HCCI without spark-assistance is possible for all test fuels.

In order to examine fuel effects, all three fuels are operated with the same exhaust valve opening (EVO) timing, NVO duration and 4mm valve lift. The independent parameters remaining are fuel injection timing and intake valve closing (IVC) timing as no spark was present. Because each fuel has a different propensity to auto-ignite, it is not possible to operate with constant fuel injection and IVC timing for all fuels. Late or retarded IVC timing has the effect of reducing the effective compression ratio in the engine, and therefore retards combustion phasing. Similarly, retarding fuel injection timing has the effect of retarding combustion phasing.

Table 5 illustrates the engine settings required for each of the 3 fuels to achieve similar combustion phasing and similar maximum pressure rise rates (MPRR). IB50 exhibits the strongest tendency to auto-ignite at this condition, and therefore has the most retarded fuel injection timing. In contrast, E85 has the least tendency to auto-ignite at this condition, and therefore requires both advanced fuel injection timing and a more advanced IVC timing.

The ensemble average pressure plots are shown in fig. 4 where it can be seen that the characteristics of the combustion event are comparable for all fuels.

If we compare the operating points in table 5, we see that combustion stability is good, as quantified by COV of IMEP. Pumping work is comparable, intake temperatures are constant and exhaust temperatures are also comparable with an increase seen with E85 attributed to the higher operating load.

TABLE 5 DATA FOR OPERATING POINTS IN FIG. 4

Fuel	UTG91	IB50	E85
DI/deg ATDC	-290	-280	-320
Spark/deg ATDC	No spark	No spark	No spark
NVO/degCA	220	220	220
IVC/deg ATDC	-135	-135	-140
MPRR/kPa/degCA	618	687	603
IMEP/ bar	352	373	406
CA50/ deg ATDC	7.5	7	9
T_in/ °C	47.9	47.9	47.1
Texh/ °C	493	494	509
PMEP/ kPa	-26.8	-26.6	-27.6
IMEP COV/%	1.86	1.86	1.66

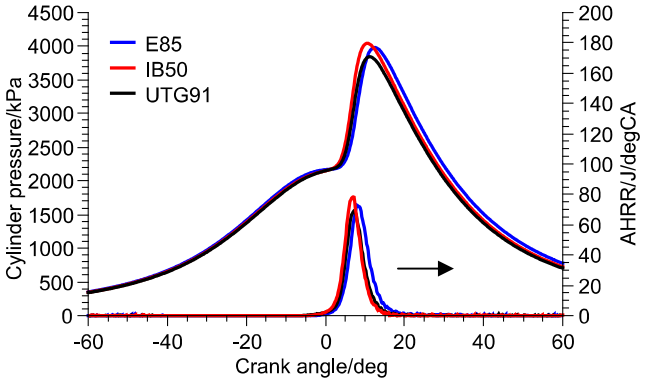

FIGURE 4 IN-CYLINDER PRESSURE: STOICHIOMETRIC OPERATION WITHOUT SPARK-ASSISTANCE (COMPARABLE PHASING AND MAXIMUM PRESSURE RISE RATE)

In summary, under stoichiometric HCCI conditions operating with an NVO duration of the order of 220degCA, the iso-butanol blend is more prone to auto-ignition than the UTG91 fuel. The E85 blend is the least prone to auto-ignition of the three fuels at this operating point. In order to achieve similar combustion phasing, modifications have to be made to fuel injection and IVC timing. Compared to UTG91, fuel injection timing is retarded for IB50 and advanced for E85. In addition, IVC is also advanced for E85.

The preceding section shows that it is possible to operate under stoichiometric conditions without spark-assistance at this

operating load. The effect of spark-assistance using the same NVO duration is dependent on fuel type. The experimental approach taken is to hold IVC constant at -135degATDC and fuel injection timing constant at -290degATDC. IB50 necessitates a retard to -280degATDC due to MPRR considerations which is attributed to NVO fuel injection characteristics. A variation of spark timing is then performed. The effects on MPRR and CA50 are shown in fig. 5 and fig. 6.

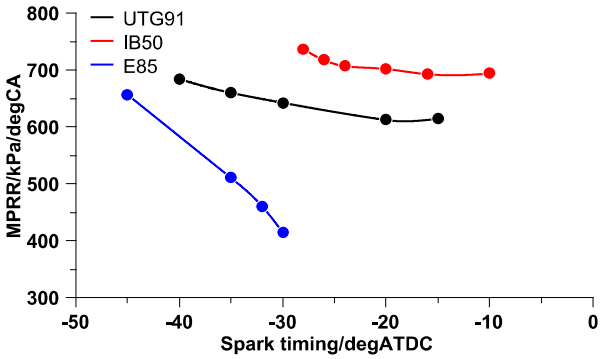

FIGURE 5 MPRR FOR SPARK TIMING VARIATION (VALVE TIMING HELD CONSTANT)

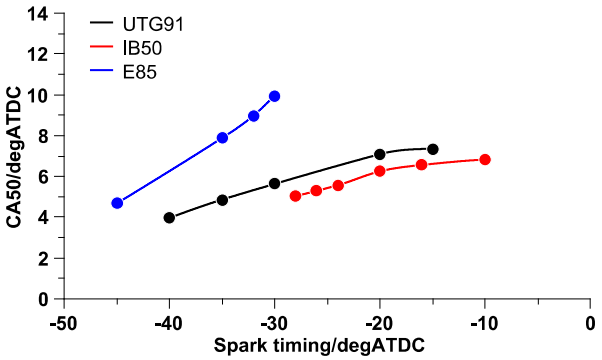

FIGURE 6 CA50 FOR SPARK TIMING VARIATION (VALVE TIMING HELD CONSTANT)

The first observation is the relative insensitivity of MPRR to spark timing with the UTG91 and IB50 fuels. The IB50 fuel also exhibits a greater MPRR than that found with UTG91. In contrast, the E85 fuel exhibits the greatest sensitivity to spark timing spanning an MPRR range from less than 400 kPa/degCA to nearly 700 kPa/degCA. In addition, for comparable combustion phasing, the E85 fuel exhibits the lowest MPRR. This emphasizes that control with spark timing alone is insufficient for all fuels, and there is a need for a combination of spark-assistance, LIVC and fuel injection timing in order to control the MPRR. Detailed studies of LIVC to reduce the MPRR further were not carried out in the present study.

The ensemble average in-cylinder pressure with comparable CA50 of ≈5degATDC is shown in fig. 7. The heat release occurring prior to the main combustion event can be attributed to a flame propagation event occurring before the volumetric auto-ignition process is instigated. This initial slow heat release (ISHR) is not exhibited in fig. 4 where spark is not used, which emphasizes the difference between the two modes of combustion. The magnitude of this ISHR is highest for E85 and lowest for IB50. This can be seen in fig. 8 where the heat release during the initial slow heat release is compared.

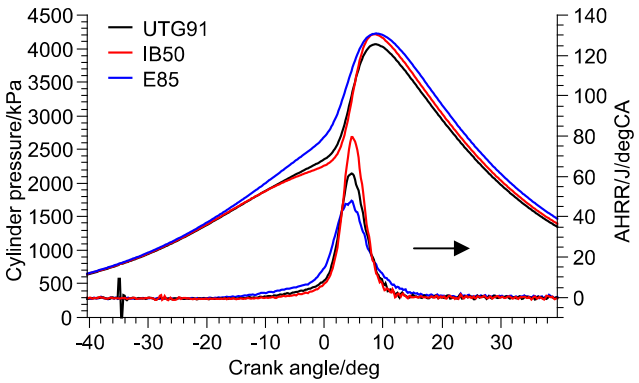

FIGURE 7 IN-CYLINDER PRESSURE: COMPARABLE COMBUSTION PHASING (VALVE TIMING HELD CONSTANT AND SPARK TIMING VARIED)

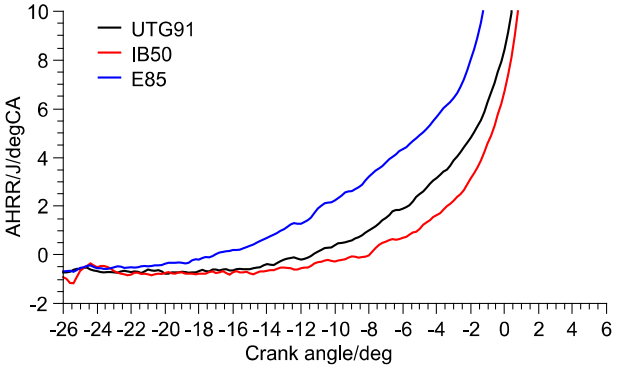

FIGURE 8 APPARENT HEAT RELEASE RATE: COMPARABLE COMBUSTION PHASING (MAGNIFICATION OF FIGURE 7)

The reason for the difference in ISHR can be attributed to the spark timing event. It is shown in the previous section that E85 possessed the lowest ignitability of the three fuels at this operating point. Therefore an advance of spark timing was required to maintain comparable combustion phasing with the IB50 and UTG91 fuels.

At the same time, both E85 and UTG91 exhibit a lower MPRR value than IB50 at this condition despite comparable phasing. Therefore the reason for the reduced MPRR cannot be attributed solely to the two-stage combustion and is also not attributed to combustion phasing in these operating points.

Operating points with comparable DI and spark timing with an identical IVC are shown in fig.9. A comparison of this heat release in fig. 10 shows that the UTG91 and IB50 fuels exhibit similar heat release characteristics whereas the E85 exhibits a transition to auto-ignition at a later crank angle position of approximately 2degATDC.

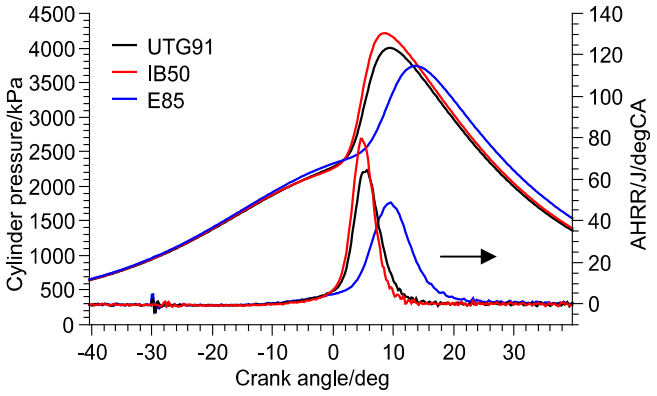

Figure 9 IN-CYLINDER PRESSURE: COMBARABLE OPERATING PARAMETERS (DI TIMING, SPARK TIMING AND INTAKE VALVE CLOSING ANGLE)

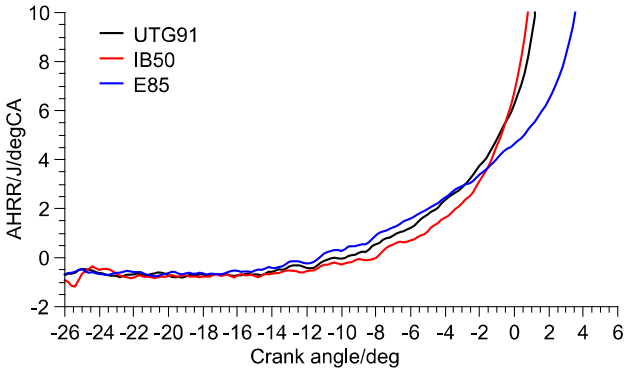

FIGURE 10 APPARENT HEAT RELEASE: COMBARABLE OPERATING PARAMETERS (MAGNIFICATION OF FIGURE 9)

In order to limit the increased MPRR exhibited with IB50, it is necessary to retard spark timing as well as DI timing. The operating parameters are shown in table 6.

TABLE 6 DATA FOR OPERATING POINTS IN FIGS. 9 & 10

Fuel	UTG91	IB50	E85
DI/deg ATDC	-290	-280	-290
Spark/deg ATDC	-30	-28	-30
NVO/degCA	220	220	220
IVC/deg ATDC	-135	-135	-135
MPRR/kPa/degCA	642	736	414
IMEP/ bar	342	360	410

Moderate Engine Loads (≈600 kPa IMEP region)

Operation at an increased load of approximately 600 kPa IMEP is achieved with an NVO duration of 160degCA. As stated earlier, NVO is held constant in order to minimize the effect of different recompression processes on the fuel matrix. It also better represents application of production-intent valvetrains possessing less flexibility than the HVA system on this research engine.

The operating range in this section is well beyond that of lean HCCI, which is limited to approximately 400 kPa IMEP. Increasing the operable load range with this mixed-mode combustion strategy has been confirmed in other studies of this combustion approach using gasoline fuel [6],[7],[8].

It is observed subjectively when operating the engine that engine noise increases in this operating region compared to the lighter load conditions. A more detailed examination of the load limits of each fuel using cyclic data and additional noise/knocking metrics is now presented by examining operating points with an MPRR of 550 +/- 20 kPa/degCA. Three measurement points, one from each of the test fuels is chosen for this analysis and is described in table 7.

TABLE 7 DATA FOR MODERATE ENGINE LOAD

Fuel	UTG91	IB50	E85
DI/deg ATDC	-290	-290	-300
Spark/deg ATDC	-22	-25	-32
NVO/degCA	160	160	160
EVO/deg ATDC	170	170	170
IVC/deg ATDC	-150	-150	-170
MPRR/kPa/degCA	530	530	560
IMEP/ bar	560	580	640
CA50/ deg ATDC	13.5	13	8.9

If we examine the engine parameters in table 7, it can be seen that for fixed NVO of 160 degCA, EVO of 170degATDC and valve lift of 6mm it is necessary to adjust the values of DI and spark timing as well as IVC depending on the fuel in order to achieve comparable values of MPRR. For the same NVO duration, the E85 fuel requires a greater advance of both spark and DI timing than either IB50 or UTG91. Therefore E85 operates with a more advanced CA50 than the other test fuels in part a consequence of the requirement for spark advance in order to overcome the reduced propensity for auto-ignition to occur. This trend is also seen with IB50 when compared with UTG91 at this operating point.

The greater propensity for the gasoline and IB50 to undergo auto-ignition also demanded that a later IVC be used to control engine noise (IVC was retarded by 20degCA compared with E85 operation). Retarded IVC reduces the amount of air breathed by the engine, which impacts IMEP because all data is collected at stoichiometric AFR conditions.

In summary, these three cases represent adjustments needed to achieve comparable levels of MPRR for the three fuels operating with an NVO duration of 160degCA. This emphasizes the significant differences between the fuel auto-ignition behavior and shows that these fuels can be accommodated by DI and spark timing adjustments in the SA-HCCI operating regime.

CYCLIC OBSERVATIONS

The MPRR, CA50, and IMEP values shown in table 7 are the mean value over 300 individual cycles. MPRR is comparable between fuels at the operating points examined. Standard deviation of MPRR is high, 2.3-2.6 bar/degCA but comparable for all fuels. Finally, the standard deviation of peak pressure does exhibit some fuel dependencies, with a minimum for UTG91 and increasing values for iso-butanol and E85.

Despite the high standard deviations for MPRR and CA50, the COV of IMEP is at or below 2%, indicating that combustion is very stable. In order to understand why the deviation of MPRR and peak pressure is somewhat elevated despite low levels of COV of IMEP it is necessary to examine the flame propagation stage of combustion.

Initial slow heat release (E85)

The E85 test point possessed an average ISHR of 41% with the highest ISHR recorded for an individual cycle of 52% and the minimum 32% during 300 cycles. 7 cycles out of 300 exhibited near zero ISHR and were comparable to HCCI combustion. A set of 10 representative consecutive cycles is shown in fig. 11. The ensemble average pressure trace is included for reference and will be referred to at a later point.

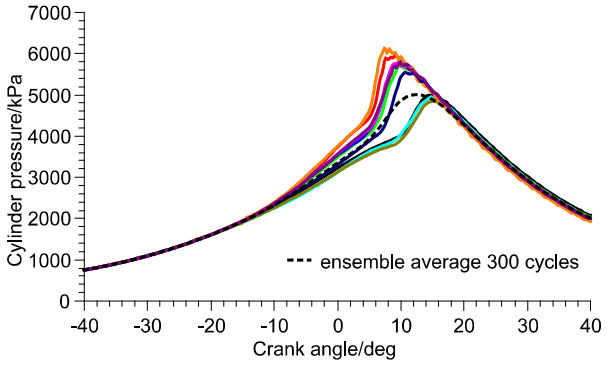

FIGURE 11 IN-CYLINDER PRESSURE MODERATE LOAD (E85)

If we examine the cumulative heat release, shown in fig. 12, for these cycles we see that the magnitude of heat release (shown by the marked points on the figure) when transition from flame propagation heat release to auto-ignition heat release occurs, is relatively constant. Nevertheless combustion phasing variation between cycles does exist at the onset of auto-ignition.

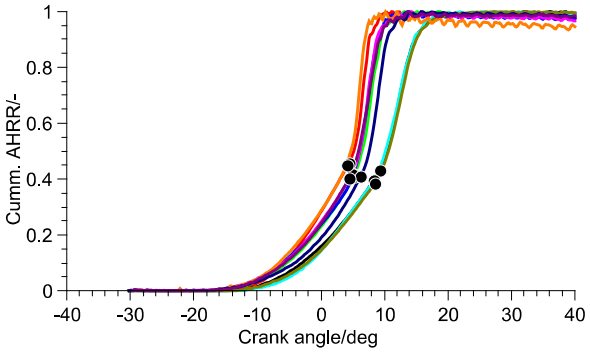

FIGURE 12 CUMMULATIVE HR MODERATE LOAD (E85)

The combustion phasing as well as the peak cylinder pressure can be seen to vary between cycles in fig. 11. If the peak cylinder pressure and pressure rise rate are plotted along with the crank angle location of the ISHR inflection point which we can denote as the end of the flame propagation event (EO_ISHR) shown by the black circles shown in fig. 12., we observe that these phenomena are related, shown in fig. 13.

When the end of ISHR occurs earlier, the peak pressure and the pressure rise rate of that cycle are increased. The most advanced EO_ISHR in this set corresponds with cycle 139 shown as the orange colored trace in fig. 11 and fig. 12. It can also be seen that HCCI knock occurs just after the peak pressure location in the cycles with the most advanced value of EO_ISHR and resulting peak pressure, as is indicated by the oscillations in the pressure trace and in the cumulative heat release in fig. 11 and fig. 12.

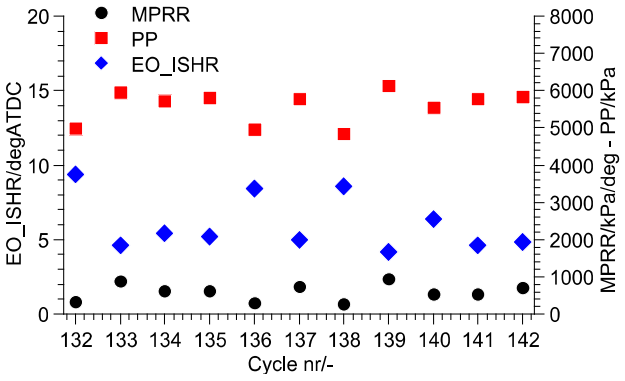

FIGURE 13 CYCLIC VARIATION OF MAXIMUM PRESSUR RISE RATE (MPRR), PEAK PRESSURE (PP) AND END OF INITIAL SLOW HEAT RELEASE (EO_ISHR) (E85)

Initial slow heat release (IB50)

The IB50 fueled operating point exhibits a reduced magnitude of ISHR compared with E85 shown by the in-cylinder pressure and cumulative heat release. The average ISHR for IB50 is 24%.The highest ISHR recorded for an individual cycle being 40% and the minimum 13% during 300 cycles. 13 cycles out of 300 exhibited near zero ISHR and were comparable to HCCI combustion.

The spark timing for IB50 is more retarded than for E85, from -32 to -25deg ATDC due to MPRR being increased with more advanced spark timing. A greater proportion of the heat release can be attributed to auto-ignition in this case and individual cycles possessing high MPRR and ringing can be seen.

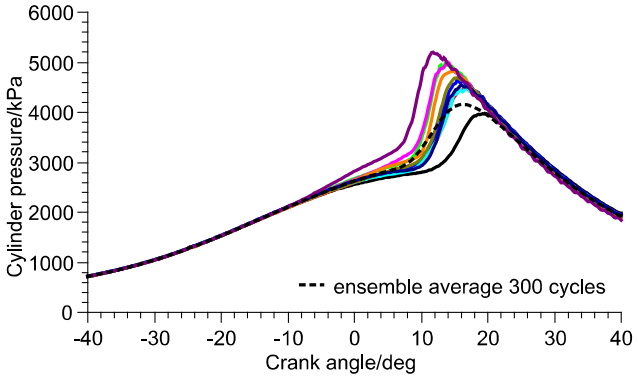

FIGURE 14 IN-CYLINDER PRESSURE MODERATE LOAD (IB50)

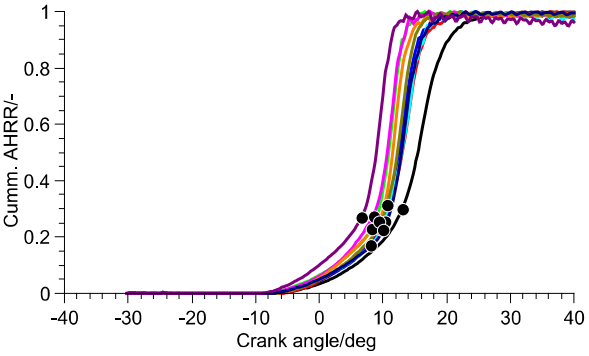

FIGURE 15 CUMMULATIVE HR MODERATE LOAD (IB50)

The cyclic values of MPRR, PP and EO_ISHR are shown in fig. 16. The same relation between cycles with increased MPRR and PP with an advanced EO_ISHR can be seen. It can also be seen that the combustion phasing is retarded when compared with E85 in fig. 14. This emphasizes another observation that the E85 fuel tended to exhibit a lower MPRR during the auto-ignition phase than the other fuels at the operating points discussed. This meant that E85 could operate with a more advanced combustion phasing while exhibiting comparable values of MPRR.

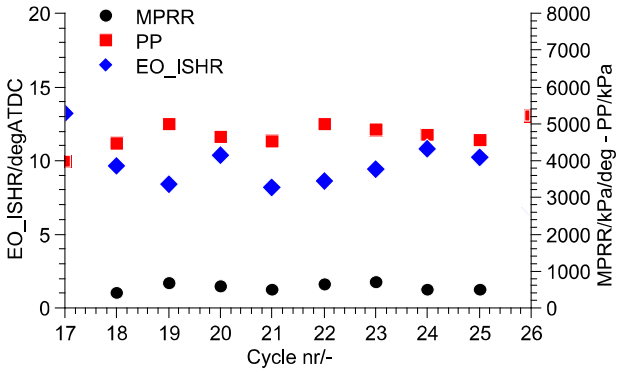

FIGURE 16 CYCLIC VARIATION OF MAXIMUM PRESSUR RISE RATE (MPRR), PEAK PRESSURE (PP) AND END OF INITIAL SLOW HEAT RELEASE (EO_ISHR) (IB50)

Initial slow heat release (UTG91)

The average ISHR for UTG91 is 22%. The highest ISHR recorded for an individual cycle being 47% and the minimum 12% during 300 cycles. This is the lowest of range of the three fuels at this operating point and is thought to be a consequence of the retarded spark timing, leading to the smallest ISHR value. 10 cycles out of 300 exhibited near zero ISHR and were comparable to HCCI combustion.

As discussed, the spark advance was chosen in order to maintain combustion stability (a retard leading to an increase in instability) and at the same moderate the MPRR value (an advance leading to an increase in MPRR). Within these constraints the UTG91 fuel required the most retarded spark timing. The in-cylinder pressure and the cumulative heat release curves are shown in, fig. 17 and fig. 18. The inflexion point is shown on fig. 18.

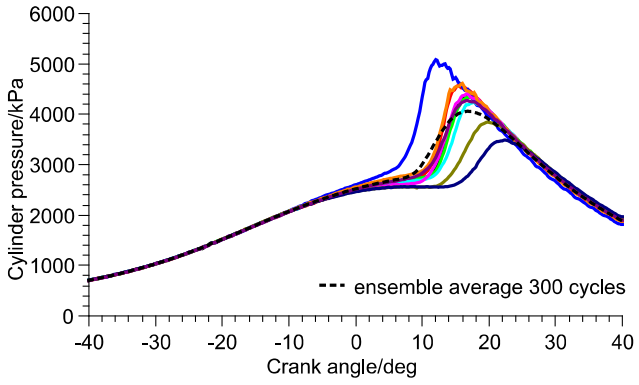

FIGURE 17 IN-CYLINDER PRESSURE MODERATE LOAD (UTG91)

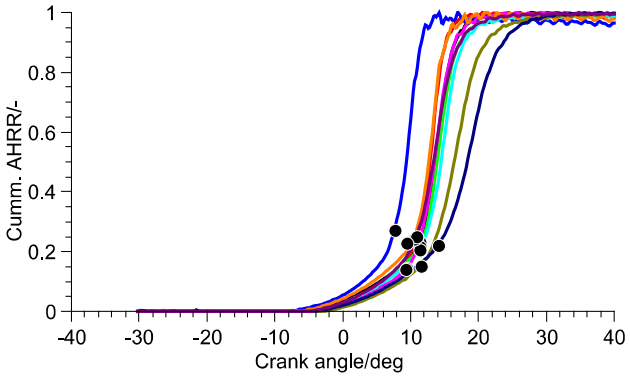

FIGURE 18 CUMMULATIVE HR MODERATE LOAD (UTG91)

The relationship between advance of EO_ISHR and peak pressure is shown in the same manner as the other fuels in fig. 19. Cycles display more advanced slow heat release leading to the greatest peak pressure and rate of heat release during the subsequent auto-ignition phase.

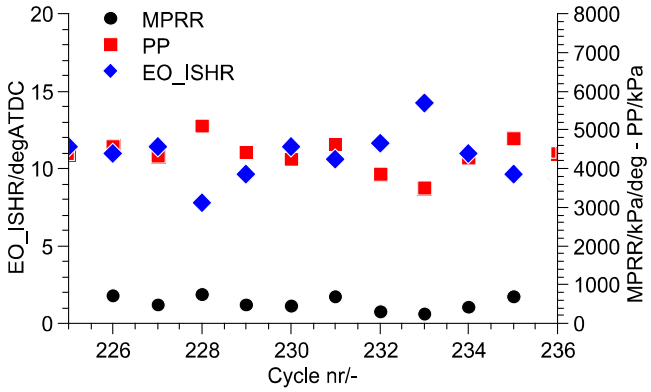

FIGURE 19 CYCLIC VARIATION OF MAXIMUM PRESSUR RISE RATE (MPRR), PEAK PRESSURE (PP) AND END OF INITIAL SLOW HEAT RELEASE (EO_ISHR) (UTG91)

COMBUSTION NOISE METRICS

In addition to using the maximum pressure rise rate averaged over 300 cycles we can examine the combustion noise characteristics using ringing intensity correlations.

Operation with UTG91 fuel discussed in the last section showed in fig. 19, that cycle 228 was a good representation of cycles that possess a MPRR higher than the mean average. The pressure wave oscillations occurring just after the peak pressure point exhibit increased amplitude correlating with the increased MPRR for this cycle.

If we use the ringing intensity correlation presented in [18], we must define the value of the factor ß (ratio of the pressure amplitude to the pressure rise rate). It is generally assumed to take a value of 0.05 which was the value calculated for the engine in [18].

Using ß = 0.05, the RI for 300 cycles is 6.8MW/m^2. A later investigation of HCCI noise metrics [19] found values of 5.3MW/m^2 for slight knock, 10.2 MW/m^2 for persistent knock and 55 MW/m^2 for heavy knock for the engine used in their studies. In those terms, the mean RI calculated in the present study at this operating point would denote a level of knock well below persistent but within the slight knock regime. This correlates well with observations while operating the engine that an increased level of engine noise is perceived at this engine operating point.

However it must also be considered that sensitivity to ß and its effect on the RI value is not insignificant. A study of a comparable combustion mode [11] found that the calculated values of the beta factor were reduced for the engine used in that study (a mean value of 0.0265 was found, with many cases possessing a beta below 0.02).

If we take the example of cycle 228 in the present work, possessing an increased pressure rise rate and noticeable ringing the beta value calculated from this data would be less than 0.02 leading to a reduction in RI when compared with the assumption that ß=0.05.

In addition it must also be considered that the presence of pressure oscillations in the cylinder pressure trace is noticeable in only a minority of the 300 cycles. A more detailed discussion of this characteristic is beyond the scope of this paper.

Despite calculated ß values being used in some studies, a fixed value of ß=0.05 was assumed in the remainder of this paper for consistency with values published elsewhere.

The same operating point in terms of the metric proposed in [19], exhibits a pressure rise rate of 2.8 MPa/ms which is lower than the knock limit of 5 MPa/ms proposed using the engine configuration used in that study.

To summarize, the following noise metrics were calculated for the operating points discussed:

1) 300 cycle averaged MPRR (calculated for each cycle)

2) Ringing intensity using MPRR from 1) and ß=0.05

3) Ensemble MPRR (the maximum rate of pressure rise w.r.t. time calculated from the 300 cycle ensemble averaged pressure trace.)

4) Ringing intensity using MPRR from 3) and ß=0.05

The results are presented in table 8.

TABLE 8 NOISE METRICS AT MEDIUM LOAD

Fuel	MPRR/ kPa/degCA	RI/ MW/m^2	RI/ MW/m^2 (ensemble)	MPRR/ MPa/ms (ensemble)	IMEP/ kPa
UTG91	530	6.8	1.3	2.8	560
IB50	530	6.8	1.0	2.4	580
E85	560	7.6	1.1	2.6	640

This suggests that in terms of ringing intensity, the engine operation is now operating at or above the slight knock regime (assuming ß=0.05) and in terms of ensemble MPRR the engine operation is below the subjective 5 MPa/ms limit discussed in [19]. What is also shown is the significant difference between the RI value when an ensemble pressure trace is used.

This is due to two reasons, firstly that an ensemble average of mixed-mode combustion where some variation of combustion phasing occurs may lead to a result that is not representative (as observed in the ensemble average pressure traces presented earlier), and secondly, any reduction of MPRR that results will affect the RI value more significantly due to the second order term containing the dP/dt relation.

Increase of operating load (600-700kPa IMEP region)

In order to evaluate the operating load limit, the NVO duration is reduced with a corresponding increase in fueling to maintain stoichiometric operation. All other parameters were unchanged from those shown in table 7.

Fueling is increased and NVO decreased until 601kPa and 627kPa IMEP were reached with UTG91 and IB50 respectively. At these operating points shown in table 9, the MPRR calculated for each cycle then averaged over 300 cycles was of the order of 550-580 kPa/degCA.

The ensemble average MPRR remains at approximately 2.5 and the RI calculated for each cycle then averaged over 300 cycles was in the 7.4-8.1 MW/m^2 range (assuming ß=0.05). This would be quantified as between slight knock and persistent knock in [19]. Combustion stability as quantified by COV of IMEP remained within an acceptable limit of 2-3%.

The ensemble MPRR remains below the 5MPa/ms limit proposed in [19]. Firstly, the limit was a subjective limit described for the engine used in [19]. Secondly, the tendency for SA-HCCI to exhibit an increased variance in pressure rise rate between cycles is likely to be obscured by the use of the ensemble average pressure curve as already mentioned. Nevertheless what is clear is that the high load operating range is limited by ringing phenomena and some cyclic variation in MPRR.

TABLE 9 NOISE METRICS AT INCREASED LOAD (UTG91 AND IB50)

Fuel	UTG91	IB50
MPRR/kPa/degCA	555	578
RI/ MW/m^2	7.4	8.1
NVO/degCA	148	148
RI/MW/m^2 (ensemble average)	0.96	1.05
MPRR/ MPa/ms (ensemble average)	2.4	2.5
IMEP/ bar	601	627
CA50/ deg ATDC	14.2	12.7

Different strategies may of course mitigate high load pressure rise rate limitations to some extent. For example the use of asymmetric valve lifts, advanced fuel injection timing and very late IVC to reduce the effective compression ratio. The detrimental effect on fuel consumption of some of these strategies must be considered and will ultimately achieve increases of load of the order of less than 1 bar IMEP over what has been measured here.

The NVO variation for E85 is shown in table 10. Here it can be seen that the ringing intensity is elevated into the persistent knock regime as NVO is reduced to 146degCA but that the ensemble average MPRR is below the 5MPa/ms discussed in [19] at the highest load of 706kPa with the lowest NVO duration.

TABLE 10 NOISE METRICS AT INCREASED LOAD WITH NVO VARIATION (E85)

NVO duration/degCA	160	150	146
MPRR/kPa/degCA	561	624	696
RI/ MW/m^2	7.6	9.3	11.7
RI/MW/m^2 (ensemble average)	1.05	1.3	1.9
MPRR/MPa/ms (ensemble avg.)	2.5	2.8	3.4
IMEP/ bar	639	685	706
CA50/ deg ATDC	8.8	7.9	6.9

It is also noted that for comparable values of MPRR, E85 is operated with an advanced CA50 when compared with UTG91 and IB50. This is a consequence of the advance of spark timing used with E85 with the UTG91 fuel operating with the most retarded spark timing. The E85 fuel is sensitive to spark timing retard leading to unstable combustion. This is also true of the UTG91 and to a lesser extent the IB50 blend; however spark advance led to a rapid increase of MPRR with the UTG91 and IB50 fuels.

For further load increase with a reduction in NVO to values less than 146-148degCA the quantity of fuel consumed by the propagating flame is increased before the conditions for auto-ignition are met which leads to ISHR values above 50%. At that

point the combustion is more comparable to dilute, spark-ignited combustion than to spark-assisted HCCI. What appears to resemble SI knock was also found to increase incrementally [8] once the flame-propagated phase becomes dominant.

Further investigation into the characteristics of operation where the ISHR value exceeds 50% was beyond the scope of this study.

INDICATED THERMAL EFFICIENCY

Figure 20 shows indicated thermal efficiency for UTG91, IB50 and E85 operating under conventional SI engine conditions. All fuels exhibit a similar pattern of increasing efficiency with increasing load. This is the expected trend and can be attributed to a reduction in pumping losses at higher load as well as reduced heat losses as a fraction of the total fuel energy and faster combustion.

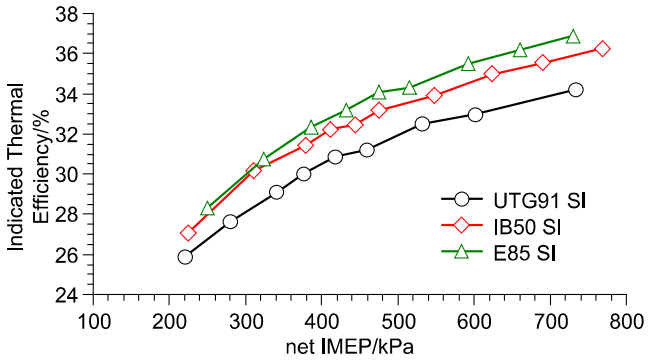

FIGURE 20 INDICATED THERMAL EFFICIENCY (SI)

It can also be seen that indicated thermal efficiency is highly dependent on the fuel type, with E85 having the highest thermal efficiency, followed by IB50, with gasoline possessing the lowest efficiency. The efficiency increase for E85 is consistent with previous engine studies [20],[16],[21] as well as vehicle studies [22],[23]. While the reason for the higher efficiency isn't completely clear, it is commonly attributed to reduced heat losses during combustion due to the lower combustion temperatures. For example, the exhaust manifold temperature is approximately 20-25 Celsius lower for E85 compared to UT91 for the SI data shown in fig. 20.

The efficiency of IB50 throughout the load range lies between that of UTG91 and E85. This finding is not surprising because IB50 contains 50 vol% gasoline, more than the 15 vol% contained in E85. In addition, iso-butanol has a higher MW alcohol than ethanol with a lower oxygen mass fraction, which may cause it to behave more similarly to hydrocarbon fuels. Thus, its efficiency performance is between UTG91 and E85.

The efficiency of each of the fuels under SA-HCCI conditions is compared to the efficiency of SI combustion with UTG91 in fig. 21. The SA-HCCI combustion regime provides a marked efficiency advantage for all fuels. Compared to the reference case of SI combustion with UTG91, thermal efficiency is increased up to 3 percentage points for UTG91 and IB50 under SA-HCCI conditions and by 5 percentage points for E85.

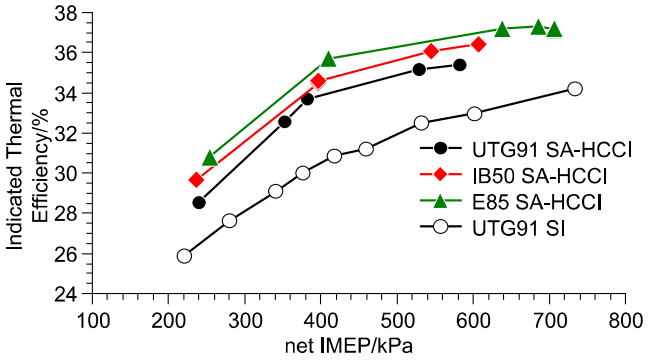

FIGURE 21 INDICATED THERMAL EFFICIENCY (SA-HCCI)

Similar efficiency increases were shown for this combustion mode in a previous study by the authors [7], where the higher efficiency was primarily attributed to a reduction in pumping losses and a decrease in combustion duration. The findings here demonstrate that the efficiency advantage of this combustion mode isn't specific to gasoline, or to fuels that have the same auto-ignition characteristics. Instead, large efficiency increases are also seen for E85 and IB50 despite their differing propensities to auto-ignite, and the resulting variability in engine control parameters, such as fuel injection timing and IVC timing.

To summarize, both E85 and IB50 exhibit higher efficiency under conventional SI conditions. The higher efficiency for E85 is consistent with published literature. All fuels exhibit a substantial efficiency increase when operating under SA-HCCI. The efficiency of E85 operating under SA-HCCI conditions is as much as 5 percentage points higher than UTG91 under conventional SI conditions.

DISCUSSION

In this study, the applicability of a 50% volume blend of gasoline and iso-butanol as well as a high volume blend of ethanol, E85 have been examined in a mixed-mode SA-HCCI combustion regime. It is possible to operate the engine stoichiometrically at 2000rpm from a low load limit of 250kPa IMEP up until the high load limit of 600-700kPa depending on fuel characteristics and the nature of combustion noise limitation applied.

It could be seen that in order to control charge air mass, and consequently operating load, it is necessary to adjust the NVO duration. This meant load increase led to a reduced propensity for the conditions for auto-ignition to occur. At the same time, the proportion of combustion associated with a spark ignited propagating flame increased. The interaction between this fundamental characteristic of naturally-aspirated SA-HCCI and the properties of the respective fuels led to a number of observations

FUEL EFFECTS

The propensity for auto-ignition to occur is lowest for E85 at all the operating loads and conditions discussed in the results section.

At increased operating loads, where a reduction in NVO is required, the iso-butanol blend showed evidence of a reduced propensity to auto-ignition compared with UTG91 which is the fuel most likely to undergo auto-ignition.

The first consequence of this is a requirement for combustion to be retarded for UTG91 and IB50 fuels in order to control combustion noise. This is done by retarding spark timing. The second consequence is a reduction in ISHR as spark is retarded, which resulted from less fuel being consumed by a propagating flame before volumetric combustion is initiated. These were the reasons for the advanced combustion phasing and raised ISHR with E85, with phasing retard and ISHR decrease seen for the iso-butanol blend and UTG91 fuels.

At lower operating loads, with a greater NVO duration and increase in volumetric combustion, a slightly different trend is observed. At an operating load of 380-400kPa IMEP with an NVO duration of 220degCA the propensity for auto-ignition is lower for E85 than for UTG91. The iso-butanol blend exhibited an increased MPRR compared to UTG91 when operating with comparable combustion phasing.

Although not shown in this paper for reasons of brevity, it is also found that at the lowest operating load of approximately 250kPa IMEP, E85 possessed atypical behavior with a more advanced combustion phasing than gasoline for the same NVO duration. Similar findings for alcohols during HCCI combustion were discussed in [24]. For the reasons outlined, E85 did not pose a low-load stability limit compared with UTG91. In the present study at 2000rpm, 250kPa IMEP operation exhibited a COV of IMEP of 3% or less.

Of course, the RON and MON ratings of a fuel do not fully describe the propensity for auto-ignition. These octane tests differ from that found in real engines and also from that found during stoichiometric HCCI combustion. Additionally the octane sensitivity or the difference between RON and MON values for the fuels in this study must also be considered when evaluating the combustion characteristics.

In terms of auto-ignition quality [25] or ignitability [26] it has been found that an octane index (OI) represents this quality well for HCCI combustion [25]:

$$OI = K*MON + (1-K)*RON \qquad (1)$$

The constant K depends not on the fuel properties but on the pressure and temperature evolution of the unburned gas. It is shown that the value of K is highly sensitive to the gas temperature at 15 bar during compression, T_{comp15}. Importantly in terms of the current work, these relations were observed without the application of high trapped residuals resulting from NVO.

A later study investigation NVO effects in relation to the value of K in the previous expression [27] found that several fuels possessing a wide range of octane numbers exhibited similar combustion phasing when operating with high quantities of hot trapped residual gas. This correlated well with the observation that for high values of T_{comp15}, the sensitivity of CA50 to OI is reduced.

In the current study, this observation correlates with the low load operating points which necessitated significant NVO duration. This would lead to an estimated EGR mass fraction of 55-65% and result in an elevated value of T_{comp15}. Hence the trend in CA50 at lower operating loads of octane rating not describing auto-ignition quality can be explained largely by the observations and relations developed in [25]. During the present study it is also observed that advancing fuel injection timing reduced the ignition delay. The reasons for this have been discussed in several publications [28],[29],[30],[31],[32],[33], [34]. It is generally accepted that the main mechanisms include the following:

1. Heat release resulting from partial fuel oxidation.

2. Fuel reforming leading to more reactive species being formed.

The presence of heat release during the NVO period for lean HCCI operating with an established multi-injection strategy (pilot injection before the NVO and main injection after the NVO) has been confirmed by many researchers, for example, using modeling methods [32], [29] and using experimental methods [28].

The presence of an exothermic reaction during NVO does rely on oxygen availability in the NVO period, [34]. The domination of exothermic reactions over fuel reforming is also suggested for lean HCCI at the operating points studied in [28].

The operating strategy employed here, with a single fuel injection into the NVO period and a combustion regime operating under stoichiometric conditions may well differ from these findings. Particularly in terms of fuel reforming, due to the lack of available oxygen for exothermic reactions to take place. The interaction between fuel injection timing in the NVO period with fuel composition is the subject of ongoing research.

INDICATED THERMAL EFFICIENCY

Results show that there are fuel-specific dependencies on thermal efficiency under conventional SI combustion. The baseline gasoline, UTG91, has the lowest thermal efficiency throughout the load range, followed by IB50, with the thermal efficiency of E85 being approximately 2 percentage points higher throughout the load range.

SA-HCCI combustion provides increases in thermal efficiency of up to 3 percentage points compared to SI operation of the same fuel. The higher efficiency is attributed to a reduction in pumping losses and a decreased combustion duration. The fuel-specific efficiency increases for E85 and IB50 and the efficiency increases of the SA-HCCI combustion mode are additive, so that the efficiency of E85 operating under SA-HCCI conditions is approximately 5 percentage points higher than for UTG91 operating under conventional SI combustion.

Thus, these findings here demonstrate that the efficiency advantage of this combustion mode isn't specific to gasoline, or to fuels that have the same auto-ignition characteristics. Instead, large efficiency increases are also seen for E85 and IB50 despite their differing propensities to auto-ignite, and the resulting variability in engine control parameters, such as fuel injection timing and IVC timing.

CONCLUSIONS

1) The stoichiometric SA-HCCI regime showed that an operating range from a low load of 250kPa to a high load of 600-700kPa IMEP was possible. This is a substantial increase of the HCCI operating range.

2) It was possible to operate the engine in SA-HCCI combustion mode using fuels with a wide range of properties, including a large difference in octane rating. This was enabled using variation in spark timing, DI timing and intake valve closing angle.

3) The engine-out emissions of NO_x, CO and HC are reduced with oxygenated fuels, but are sufficiently high with all fuels to require aftertreatment. The stoichiometric air to fuel ratio maintains compatibility with using conventional TWC technology to allow for very low tailpipe-out emissions at all engine loads.

4) E85 exhibited a lower auto-ignition quality when operating between 380kPa and 700kPa IMEP when compared with UTG91 gasoline and a 50% volume blend of iso-butanol with gasoline. In general, an advance of spark timing and DI timing was required with E85 to maintain optimal operation in terms of stability and combustion noise.

5) A 50% volume blend of iso-butanol and UTG91 gasoline exhibited a higher auto-ignition quality than UTG91 gasoline and E85 at 380-400kPa. At higher operating loads, the auto-ignition quality of the iso-butanol blend was more comparable with UTG91 gasoline. This was attributed to the effect of an increased NVO duration at lower loads which led to an increased RGF and compression stroke temperature. These factors can lead to the auto-ignition quality of the fuel deviating from those measured using standard RON and MON tests.

6) The propensity for E85 and to a lesser extent the iso-butanol blend to require advance of spark timing leads to an increase in the magnitude of spark ignited flame-propagation event when compared with UTG91 gasoline when operating at medium to high loads.

7) The highest operating region of 600-700kPa is limited by in-cylinder pressure rise rate considerations. Further load increase is limited by two phenomena:

a. Individual cycles possessing high rates of in-cylinder pressure rise rate corresponding with an SI event occurring with advanced combustion phasing.
b. An increase in the cyclic variability of cycles possessing high rates of pressure rise rate.

8) The effect of cyclic variability during the SI component of combustion is thought to have a significant influence on the following volumetric combustion event. This is expected to lead to cyclic variability of pressure rise rates seen at high operating loads. The reduced NVO duration necessary at these high loads increases the magnitude of SI combustion so this cyclic variability is therefore more apparent in the high load operating region.

9) Comparison of combustion noise metrics found that SA-HCCI combustion may be best evaluated using a mean average of each of the cycles in terms of both maximum pressure rise rate and ringing intensity. The use of an ensemble average of the pressure curves may lead to inconsistency due to the existence of an SI phase and a volumetric phase subject that are subject to some cyclic variability.

10) E85 and the iso-butanol/gasoline blend both produce a higher thermal efficiency than gasoline under comparable conditions during both SI and SA-HCCI combustion.

11) SA-HCCI produces a higher efficiency than conventional SI combustion for all fuels, largely attributable to reduced throttling losses and decreased combustion duration. As a result, the thermal efficiency for E85 operating under SA-HCCI conditions is approximately 5 percentage points higher than for gasoline under SI conditions.

ACKNOWLEDGMENTS

Research sponsored by the U. S. Department of Energy, Office of Energy Efficiency and Renewable Energy, Vehicle Technologies Program, under contract DE-AC05-00OR22725 with UT-Battelle, LLC.

DISCLAIMER

REFERENCES

1. U.S. Department of Energy. “Multi-Year Program Plan 2011-2015,” 2010, Energy Efficiency & Renewable Energy, Vehicle Technologies Program, Available at http://www1.eere.energy.gov/vehiclesandfuels/pdfs/program/vt_mypp_2011-2015.pdf.
2. Najt, P. and Foster, D., “Compression-Ignited Homogeneous Charge Combustion”, 1983, SAE Technical Paper 830264.
3. Koopmans, L. and I. Denbratt. "A Four Stoke Camless Engine, Operated in Homogeneous Charge Compression Ignition Mode with Commercial Gasoline". Society of Automotive Engineers, 2001, Technical Paper 2001-01-3610.
4. Urushihara, T., K. Yamaguchi , K. Yoshizawa, and T. Itoh. "A Study of a Gasoline-fueled Compression Ignition Engine – Expansion of HCCI Operation Range Using SI Combustion as a Trigger of Compression Ignition". Society of Automotive Engineers, 2005, Technical Paper 2005-01-0180.
5. Bunting, B.G. "Combustion, Control and Fuel Effects in a Spark Assisted HCCI Engine Equipped with Variable Valve Timing", Society of Automotive Engineers, 2006, Technical Paper 2006-01-0872.
6. Yun, H., N. Wermuth, and P. Najt. "Extending the High Load Operating Limit of a Naturally-Aspirated Gasoline HCCI Combustion Engine". Society of Automotive Engineers, 2010, Technical Paper 2010-01-0847.
7. Szybist, J., Nafziger, E. and Weall, A., “Load Expansion of Stoichiometric HCCI Using Spark Assist and Hydraulic Valve Actuation”, 2010, SAE Intl. J. Engines, vol3, nr2, 244-258.
8. Manofsky, L., Vavra, J., Assanis, D. and Babajimopoulos, A.,”Bridging the Gap between HCCI and SI: Spark-Assisted Compression Ignition”, 2011, SAE Technical Paper 2011-01-1179.
9. Persson, H., Sjöholm, J., Kristensson, E., Johansson, B., Richter, M. and Aldén, M., “Study of Fuel Stratification on Spark Assisted Compression Ignition (SACI) Combustion with Ethanol Using High Speed Fuel PLIF”, 2008, SAE Technical Paper 2008-01-2401.
10. Persson, H., Johansson, B. and Remón, A., “The Effect of Swirl on Spark Assisted Compression Ignition (SACI)”, 2007, SAE Technical Paper 2007-01-1856.
11. Hyvönen, J., G. Haraldsson, and B. Johansson. "Operating Conditions Using Spark Assisted HCCI Combustion During Combustion Mode Transfer to SI in a Multi-Cylinder VCR-HCCI Engine", Society of Automotive Engineers, 2005, Technical Paper 2005-01-0109.
12. Kalian, N., Zhao, H. and Yang, C. "Effects of spark-assistance on controlled auto-ignition combustion at different injection timings in a multicylinder direct-injection gasoline engine", 2009, Int. J. Engine. Res., 10(3), pp 133-148.
13. “California Biobutanol Multimedia EvaluationTier I Report”, 2010, BP & DuPont for the California EPA
14. Lange's Handbook of Chemistry, 10th Ed.
15. “Internal Combustion Engines and Air Pollution,” Obert, E.F., 3rd Edition, Intext Educational Publishers, 1973.
16. Nakata, K., Utsumi, S., Ota, A., Kawatake, K., Kawai, T. and Tsunooka, T., “The Effect of Ethanol Fuel on a Spark Ignition Engine”, 2006, SAE Technical Paper 2006-01-3380.
17. Persson, H., Pfeiffer, R., Hulqvist,A., Johansson, B., and Ström, H., "Cylinder-to-Cylinder and Cycle-to-Cycle Variations at HCCI Operation With Trapped Residuals". Society of Automotive Engineers, 2005, Technical Paper 2005-01-0130.
18. Eng, J., “Characterization of Pressure Waves in HCCI Combustion”, 2002, SAE Technical Paper 2002-01-2859.
19. Andreae, M., Cheng, W., Kenney, T. and Yang, J., “On HCCI Engine Knock”, 2007, JSAE/SAE Technical Paper 20077115/2007-01-1858.
20. Nakama, K., J. Kusaka, Y. Daisho. "Effect of Ethanol on Knock in Spark Ignition Gasoline Engines." Society of Automotive Engineers, 2008, Technical Paper 2008-32-0020.
21. Szybist, J., Youngquist, A., Wagner, R., Foster, M., Moore, W. and Confer, K., “Investigation of Knock Limited Compression Ratio of Ethanol Gasoline Blends”, 2010, SAE Technical Paper 2010-01-0619.
22. West, B.H., López, A.J., Theiss, T.J., Graves, R.L., Storey, J.M., and Lewis, S.A., “Fuel Economy and Emissions of

the Ethanol-Optimized Saab 9-5 Biopower.", 2007, SAE Technical Paper 2007-01-3994.
23. Datta, R., Maher, M., Jones, C., and Brinker, R. "Ethanol – the primary renewable liquid fuel." Journal of Chemical Technology & Biotechnology, 2011, v. 86 pp. 473-480.
24. Xie, H., Wei, Z., He, B. and Zhao, H.,"Comparison of HCCI Combustion Respectively Fueled with Gasoline, Ethanol and Methanol through the Trapped Residual Gas Strategy", 2006, SAE Technical Paper 2006-01-0635.
25. Kalghatgi, G., "Auto-Ignition Quality of Practical Fuels and Implications for Fuel Requirements of Future SI and HCCI Engines", 2005, SAE Technical Paper 2005-01-0239.
26. Farrell, J. and Bunting, B., "Fuel Composition Effects at Constant RON and MON in an HCCI Engine Operated with Negative Valve Overlap", 2006, SAE Technical Paper 2006-01-3275.
27. Risberg, P., Kalghatgi, G.. and Ångstrom, H., "The Influence of EGR on Auto-ignition Quality of Gasoline-like Fuels in HCCI Engines", 2004, SAE Technical Paper 2004-01-2952.
28. Arning, J., Ramsander, T. and Collings, N., "Analysis of In-Cylinder Hydrocarbons in a Multi-Cylinder Gasoline HCCI Engine Using Gas Chromatography", 2009, SAE Technical Paper 2009-01-2698.
29. Aroonsrisopon, T., Nitz, D., Waldman, J., Foster, D. and Iida, M., "A Computational Analysis of Direct Fuel Injection During the Negative Valve Overlap Period in an Iso-Octane Fueled HCCI Engine", 2007, SAE Technical Paper 2007-01-0227.
30. Fitzgerald, P. and Steeper, R.,"Thermal and Chemical Effects of NVO Fuel Injection on HCCI Combustion", 2010, SAE Technical Paper 2010-01-0164.
31. Urushihara, T., Hiraya, K., Kakuhou, A. and Itoh,T., "Expansion of HCCI Operating Region by the Combination of Direct Fuel Injection, Negative Valve Overlap and Internal Fuel Reformation", 2003, SAE Technical Paper 2003-01-0749.
32. Koopmans, L., Ogink, R. and Denbratt, I., "Direct Gasoline Injection in the Negative Valve Overlap of a Homogeneous Charge Compression Ignition Engine", 2003, JSAE/SAE Technical Paper 20030195/2003-01-1854.
33. Wermuth, N., Yun, H. and Najt,P., "Enhancing Light Load HCCI Combustion in a Direct Injection Gasoline Engine by Fuel Reforming During Recompression", 2009, SAE Technical Paper 2009-01-0923.
34. Song, H., Padmanabhan, A., Kaahaaina, N. and Edwards, C., "Experimental study of recompression reaction for low-load operation in direct-injection homogeneous charge compression ignition engines with n-heptane and i-octane fuels", Int J. Engine Res. Vol 10, 2009.
35. Persson, H., A. Hultqvist, B. Johansson, and A. Remón. "Investigation of the Early Flame Development in Spark Assisted HCCI Combustion Using High Speed Chemiluminescence Imaging", Society of Automotive Engineers, 2007, Technical Paper 2007-01-0212.

NOMENCLATURE

ATDC	After top dead centre
CA50	Crank position at 50% of cumulative apparent heat release
COV	Coefficient of variance
DI	Direct injection
EO_ISHR	End of the initial slow heat release phase
HCCI	Homogeneous charge compression ignition
ISHR	Initial slow heat release
IVC	Intake valve closing
IB50	50/50 volume blend of iso-butanol and gasoline
$ISNO_x$	Indicated specific NO_x emissions
ISHC	Indicated specific HC emissions
LTC	Low temperature combustion
LIVC	Late intake valve closing
MPPR	Maximum pressure rise rate
NVO	Negative valve overlap
RGF	Residual gas fraction
RI	Ringing intensity
SA-HCCI	Spark-assisted homogeneous charge compression ignition
SI	Spark ignition
UTG91	Unleaded test gasoline
W.R.T	With respect to

ANNEX A

CALCULATIONS

COMBUSTION NOISE AND RINGING INTENSITY

The following equation shows a widely used ringing intensity correlation [18]:

$$RI = \frac{1}{2\gamma} \frac{\left[\beta\left(\frac{dP}{dt}\right)_{\max}\right]^2}{P_{\max}} \sqrt{\gamma R T_{\max}} \qquad (1)$$

The ratio of specific heats, γ, is calculated for each cycle using the compression stroke gradient of a logarithmic pV diagram. The gas constant, R assumed a value of 287 J/kgK and the bulk gas temperature is assumed arbitrarily to be 2000K, representing a combustion regime possessing some extent of SI combustion with elevated NO_x emissions forming at local temperatures in excess of 2000K. Detailed calculation of the in-cylinder temperature considering the trapped residual mass, fuel properties and fuel injection vaporization effects were beyond the scope of this paper.

It is worth noting that the sensitivity to the values of gamma, R and T_{max} are reduced when compared with the value of P_{max} and particularly to $(dP/dt)_{max}$ and beta due to the second order term in the equation.

For example a simplified version of this relation is used in [6] where the variables MPRR, engine speed and peak pressure are used along with a term that appears to lump the values of T_{max}, gamma and R as a constant term for all measurements.

In this paper the relation between the maximum pressure rise rate and the peak amplitude of pressure oscillations, ß, is calculated when stated using band-pass filtered in-cylinder pressure data with 4kHz to 25kHz pass frequencies. A fixed value of 0.05 is also used when indicated in the text.

Finally, in the present paper, the values of MPRR and RI were calculated for each cycle. Then the mean average of 300 cycles is taken.

In addition another approach proposed in [19] is also considered. That is to quantify the maximum peak pressure rise rate in terms of the pressure gradient with respect to time rather than crank angle, effectively considering engine speed as a defining factor. This metric is applied to the average ensemble in-cylinder pressure and not to individual cycles:

$$Knock\ \ threshold = \left(\frac{dP}{dt}\right)_{\max} \qquad (2)$$

INITIAL SLOW HEAT RELEASE

The metric proposed in [11] is used in this work. In summary, the initial slow heat release (ISHR) is the ratio of the cumulative heat release $Q_{threshold}$ at the end of the flame propagation event to the total cumulative heat release Q_{max}:

$$ISHR = \frac{Q_{threshold}}{Q_{\max}} \qquad (3)$$

In order to quantify the point of transition it is necessary to make a simplifying assumption when no optical access is available. It is assumed that the inflexion point in the apparent heat release rate indicated this transition in the same manner as [35]. By taking the 2nd derivative of the apparent heat release rate it is possible to identify this inflexion point as the first peak which allows a determination of the $Q_{threshold}$ at that crank angle position. This allows cyclic determination of the ISHR value and location to be determined.

An additional metric used in the body of this text is the crank angle position of the inflexion point i.e. the point at which the transition from a flame propagation combustion event to an auto-ignition event was assumed to occur.

$$\text{ISHR inflexion point} = EO\_ISHR \qquad (4)$$